Cyclic Yield Reversal in Steel Building Connections

EGOR P. POPOV AND R. BRUCE PINKNEY

For the most part, plastic analysis and design have in the past been directed toward the study of proportional, monotonically increasing loading to failure. This type of loading is not entirely realistic for many applications, however. The concepts of a shakedown analysis,[5,7,23] while enlarging the scope of plastic analysis, result in a structure which ultimately responds elastically, after a few cycles of inelastic action. Severe earthquakes, on the other hand, may induce considerable repeated inelastic action in a structure, especially at the joints. This has motivated study of steel members and connections subjected to repeated and reversed loading. Except for an earlier paper[3] by Bertero and Popov, no tests of this type appear to have been conducted in the United States, although intensive research into the problem has been carried out in Japan.[10,18]

Described herein are tests of 24 connection specimens subjected to various cyclic, quasi-static loading sequences. In addition to the behavior and the manner of failure of the beams and their connections to the columns, the hysteretic response of the beams under repeated and reversed loadings received particular attention.

Detailed results of this experimental program may be found in Refs. 20 and 21.

SELECTION AND DESIGN OF SPECIMENS

A beam size of W8×20 was used throughout this series of experiments. The proportions of this section are such that the b/t ratio is similar to that of representative floor beams used in high-rise steel buildings. Although this member has a depth of only about one-third that of beams used in actual construction, it is sufficiently large to require no specialized fabrication procedures. The beam was attached as a cantilever to a short column stub, as shown in Fig. 1.

Egor P. Popov is Professor of Civil Engineering, University of California, Berkeley, Calif.

R. Bruce Pinkney is a Graduate Student and Research Assistant, University of California, Berkeley, Calif.

This paper is reprinted from the Journal of the Structural Division, ASCE, Vol. 95, No. ST3, March, 1969.

All column stubs were fabricated from W8×48 sections. This resulted in a column stub of considerable relative rigidity and minimized the rotation of the cantilever at its support. It also ensured that the mechanism would form in the beam, in accordance with current design practice.[1]

The length of the cantilever was chosen to be approximately the scaled-down half-span length of a representative prototype. The application of a concentrated reversible load at the end of the cantilever was intended to simulate the distribution of bending moment produced in a typical beam by a lateral load on a structure. This distribution neglects the effect of gravity loading.

Five different basic connection types were investigated. In three of these, designated as F1, F2, and F3, the beam was connected to the flange of the column. In the remaining two, designated W1 and W2, the beam was connected indirectly to the web of the column. All of the connection details were chosen on the basis of their practicability and their widespread use.

Connection Type F1—The simplest and perhaps most widely used flange connection is Type F1, shown in Fig. 1. The entire capacity of the member is developed by means of full-penetration single-bevel groove welds applied to both flanges and web. Since all welding is done in the field, an erection clip angle is provided for temporary bolting and as a back-up for the vertical web weld. This connection has been adopted in this paper as the standard against which other connections are compared.

Connection Type F2—Another basic flange connection is Type F2, shown in Fig. 2. In this connection, moment transfer is effected by top and bottom flange plates. The rectangular bottom plate is shop-welded to the column by means of a full-penetration single-bevel groove weld. An erection clip functions exactly as for Type F1. At erection time, the lower flange is fillet-welded to the bottom plate; the tapered top plate is groove-welded to the column and fillet-welded to the

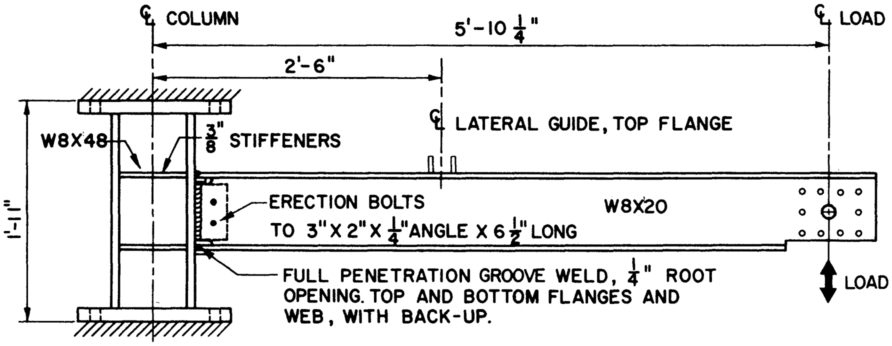

Fig. 1. Specimen Type F1.

beam flange. The top plate is so designed that at an assumed critical section, the flexural capacity of the plates, matches that of the beam section. The fillet welds are then arbitrarily extended a little beyond this design critical section.

Connection Type F3—The third flange connection, Type F3, shown in Fig. 3, makes use of high-strength bolts for stress transfer. Top and bottom flange plates and web angle are shop-welded to the column, so that only bolting is necessary in the field. In this case, the web angle is used for shear transfer as well as erection convenience. Since vertical clearance between beam and plates is ordinarily provided for ease of erection, a thin, loose filler plate is included at the top flange.

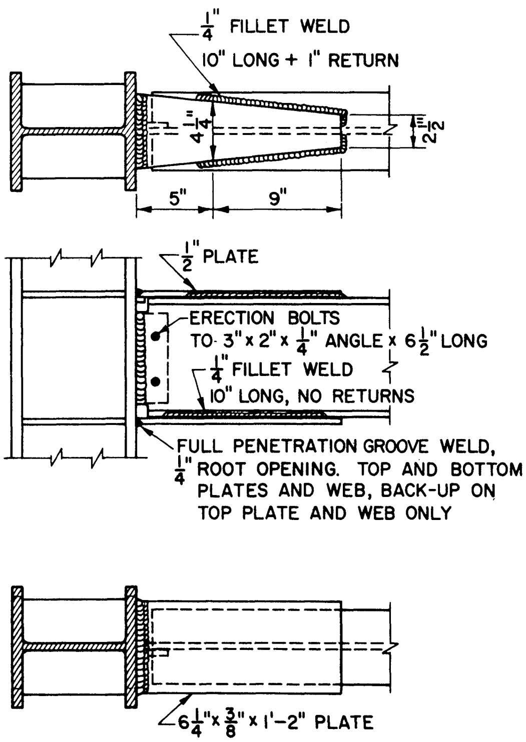

Fig. 2. Connection Type F2.

Modified Connection Types—In lateral force design of a building, beam size is frequently dictated by drift limitation rather than strength. In this case, a connection is sometimes designed to develop only the calculated stresses, and not the full strength of the connecting beam. To examine the behavior of such a connection, two specimens of Type 2 were fabricated with arbitrarily thinner connecting plates. Designated as F2A and F2B, they had top and bottom plates $\frac{1}{16}$-in. and $\frac{1}{8}$-in. thinner, respectively, than the corresponding plates of Type F2. All other details remained unchanged.

The Type F3 specimens were designed such that the capacity of the net section of the plates matched the capacity of the gross section of the beam, since there is evidence[6] that the latter may be fully developed despite the presence of holes. On the basis of the net section of the beam, however, the connection was considerably overdesigned. To compare the behavior of connections with the connecting plates designed by different criteria, therefore, two specimens of Type F3 were also fabricated with arbitrarily thinner flange plates. One of these, designated F3A, had connection plates nominally

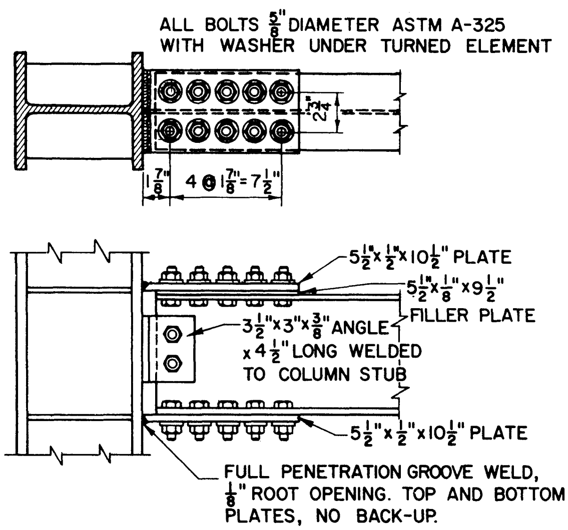

Fig. 3. Connection Type F3.

Table 1. Nominal Properties of Connection Plates

Type	Top Plate Thickness (in.)	Bottom Plate Thickness (in.)	Minimum Section Modulus[a] (in.)	Strength Factor[b]
F2	1/2	3/8	17.3	1.02
F2A	7/16	5/16	15.1	0.89
F2B	3/8	1/4	12.8	0.75
F3	1/2	1/2	17.1	1.01, 1.31[c]
F3A	7/16	7/16	15.4	0.91, 1.15[c]
F3B	3/8	3/8	13.1	0.77, 0.98[c]

[a] *At nominal critical section for type F2; at net section for type F3.*
[b] *Based on gross section of beam except as indicated.*
[c] *Based on net section of beam.*

1/16-in. thinner than those of F3. It was underdesigned on the basis of gross section, and overdesigned on the basis of net section of the beam. The other, designated F3B, had plates nominally 1/8-in. thinner than had F3. This connection was considerably underdesigned on the basis of gross section, but only slightly so on the basis of net section of the beam.

The interrelationships among the basic connections F2 and F3, and their modifications, F2A, F2B, F3A, and F3B, are summarized in Table 1. Note that these are nominal properties, based on specified dimensions, except that actual hole sizes were used for the F3 series.

Connection Type W1—The first of the web connections, Type W1, is widely used because of its simplicity. It is shown in Fig. 4. Flush stiffener plates, welded to both flanges and web of the column, provide for a direct butt-welded connection to the beam flanges. The web plate provides for temporary erection bolting and transfers shear in the completed connection through a fillet weld to the beam web.

Connection Type W2—Instead of the flush stiffener plates used in Type W1, tapered or shaped plates are sometimes used, with the idea that a gradual change in the cross section of the beam flange should reduce the effects of stress concentration. Two specimens of this type were fabricated and designated W2. Specimen W2A had a tapered plate at the top flange and a shaped plate at the bottom, as shown in Fig. 5. Specimen W2B had exactly the reverse. It was thought that in this manner a single specimen would provide information not only on the behavior of a web-connected beam, but would also point to any possible difference in performance between the two types of plate.

Fabrication of Specimens—Throughout fabrication of the specimens, an attempt was made to simulate the physical orientation and welding sequences found in actual construction. Weld back-ups were used only for field welds, and all welds which would be vertical were executed in that position. Professional inspection services were procured for many specimens.

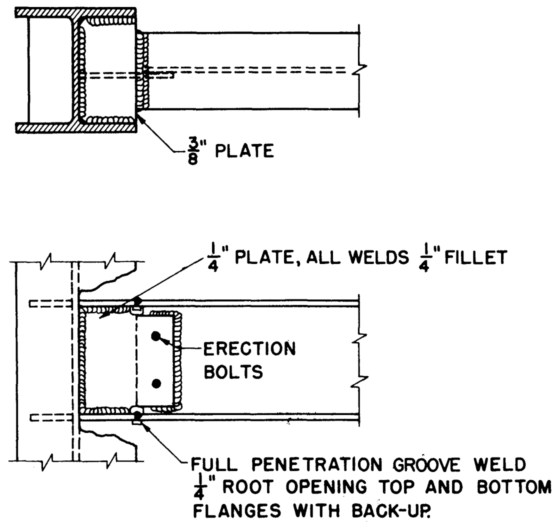

Fig. 4. Connection Type W1.

Twenty-four specimens were fabricated for the experimental program described in this report. The five basic connection types, together with the modified details for Types F2 and F3, constitute a total of nine different connections. Twenty specimens were made of ASTM A36 steel, with each type represented at least once. In addition, two each of Types F1 and F2 were made of ASTM A441 steel. The latter are identified in the sequel by the letters HS, as F1HS and F2HS, respectively. The dimensions and details for these specimens were the same as for those of A36 steel.

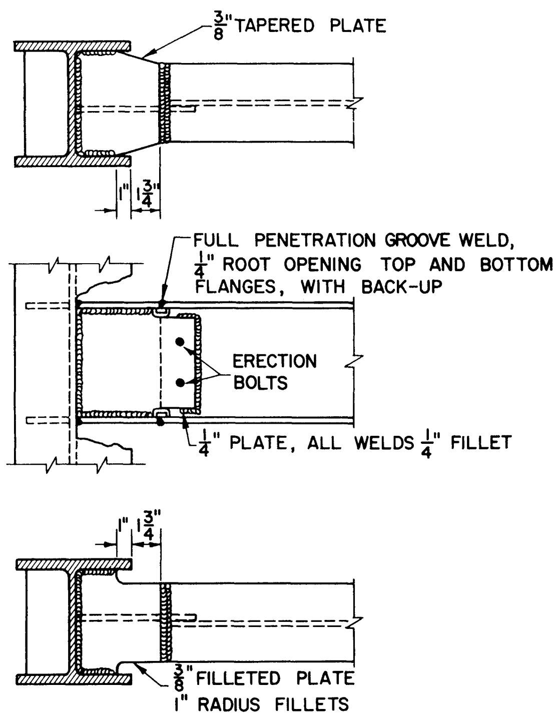

Fig. 5. Connection Type W2.

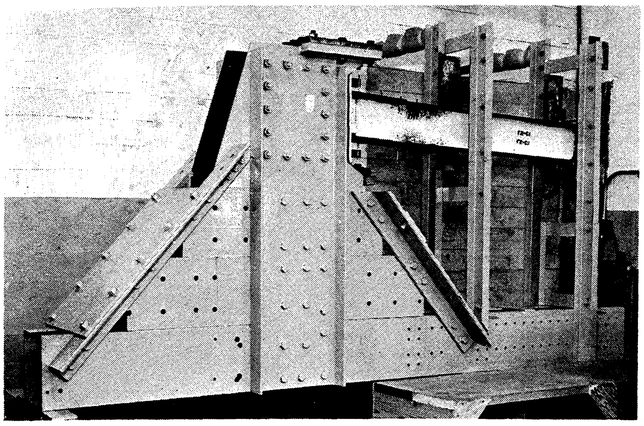

Fig. 6. Test fixture with specimen.

EXPERIMENTAL INSTALLATION

The principal features of the test fixture can be seen in Fig. 6. Provision was made to securely bolt the column stub to the frame, projecting the cantilever beam horizontally. Load was applied by means of a double-acting hydraulic cylinder.

Lateral Guides—With the end of the cantilever corresponding to the midspan of a prototype beam, it was assumed that this would represent a point of inflection in a laterally loaded structure. Since in the prototype this point would therefore not tend to buckle sideways, a guide preventing both lateral and torsional displacement was provided at the end of the specimen. Further, since the top flange of a beam in a building is typically supported laterally by the floor system, a guide preventing lateral displacement of the top flange, but permitting twisting, was provided at the middle of the cantilever.

Load Deflection Measurement—In the early experiments, the deflection of the cantilever tip (point of load) was measured intermittently by means of dial gages. The load was measured simultaneously by means of a load transducer using electrical strain gages as the sensitive elements. In subsequent tests, continuous load-deflection diagrams were automatically plotted on an XY recorder.

Strain Measurements—In many cases, single element electric strain gages were applied in the center of either the top or the bottom flange, or both, at an arbitrary distance from the face of the column stub. By connecting one of these gages to the horizontal input of an XY recorder, and the load to the vertical input, it was possible to trace graphical load-strain hysteresis loops.

In several experiments, gages were also applied in pairs directly opposite each other on the inside and outside faces of the toe of a flange. The difference in readings from such gages was found to be a sensitive indicator of the onset of local buckling.

EXPERIMENTAL PROCEDURE AND OBSERVATIONS

Static Test F1-S—Since most of the readily available experimental research on members and connections deals with a single application of a monotonically increasing load, such an experiment was performed for comparison on one of the Type F1 specimens.

To obtain an idea of the strains developed in the specimens during the experiment, the output from an electric strain gage located at 1.50 in. from the column face at the center of the top flange was monitored. At about 0.2% strain, as measured by this gage, considerable yielding of the flanges and the web had occurred, as evidenced by peeling and cracking of the whitewash applied to the specimen. Strain-hardening commenced at about 1.5% strain, causing an increase of load until the test maximum was reached at 4.5% strain. Compression flange buckling was first observed when the monitored strain was near 1%.

The behavior of the specimen in this static test was typical of the behavior many specimens previously reported in the literature.

Selection and Control of Cyclic Tests—The main purpose of these experiments, however, was to investigate the behavior of the connections during cyclically reversed loading. Hanson has demonstrated[9] that hysteresis curves induced by static testing are in good agreement with those induced by dynamic testing. The cantilever specimens were therefore subjected to a quasi-static concentrated load applied cyclically downward and upward at the tip. The selection of the maximum magnitude of the applied load, or alternatively, the applied tip deflection, is a very complex matter. There is interest in the manner of failure due to exceptionally high loads, as may well prevail in an isolated joint of a building during an earthquake. There is interest in the longevity of a connection under substantial overloads. And for purposes of dynamic analysis of the overall structural behavior of a frame, there is interest in the amount of damping which can be relied upon immediately after the elastic range is exceeded.

In an attempt to answer such questions, at least partially, a variety of cyclic loading programs was devised. In most of the tests, the program of loading was such that a sequence of increasing strain or deflection amplitudes was applied, with an arbitrary number of cycles at each amplitude. However, as such regular increments in the control parameters are not necessarily characteristic of what may occur in a real structure, other cycling programs were also used. In some cases, a constant amplitude was applied throughout the test. In others, very large displacements were applied initially, followed by moderate, stepwise increasing amplitudes. In order to identify a particular specimen, a cyclic program designation was appended to the basic specimen type, as for example, F1-C1, F2-C2, etc.

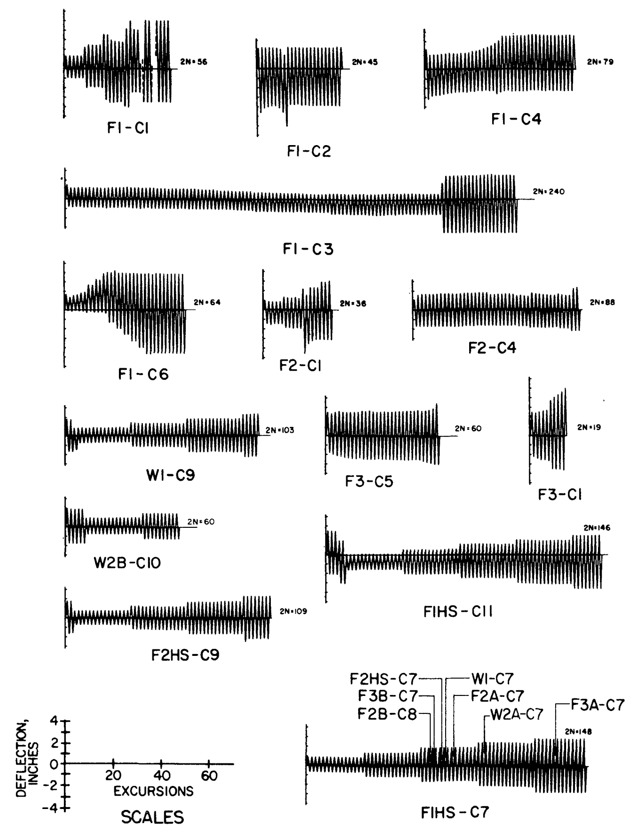

Fig. 7. Programs of cycling.

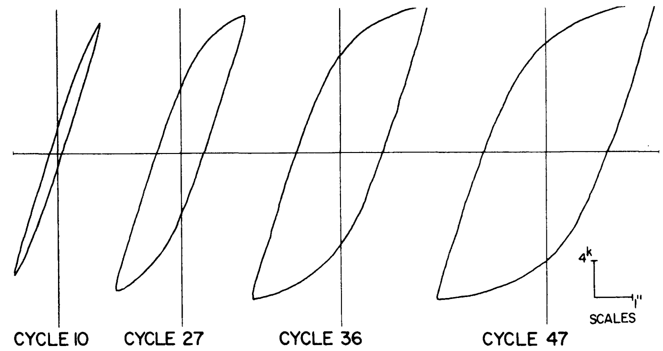

Fig. 8. Experimental Load-Deflection hysteresis loops for Specimen F1HS-C7.

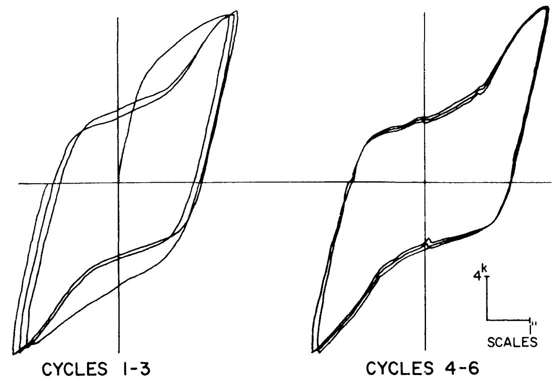

Fig. 9. Experimental Load-Deflection hysteresis loops for Specimen F3-C5.

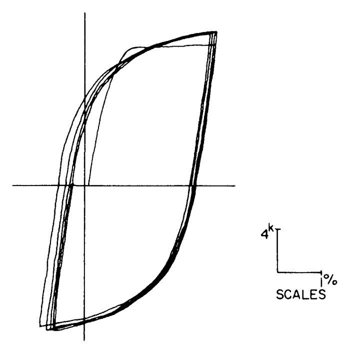

Fig. 10. Experimental Load-Strain hysteresis loops for Specimen F1-C1.

Each test began with the application of three complete cycles at a maximum nominal stess of 24 ksi. These cycles produced essentially elastic response, and served to check out the instrumentation. The schematic diagrams for almost all of the cyclic tests, exclusive of the initial elastic cycles, are shown in Fig. 7. Diagrams for specimens having the same cycle program, namely C7 and C8, have been superimposed. Each diagram clearly displays the maximum amplitudes of the tip-deflection and the number of inelastic excursions to failure. Note that the number of excursions into the plastic range is twice the number of cycles, N.

Typical Hysteresis Curves—Load-deflection data were acquired for every test with cyclically applied load. The hysteresis loops showed remarkable reproducibility during consecutive cycles of loading. As the areas enclosed by these loops correspond to the capacity of a member and its connection to absorb and dissipate energy, this indicates high dependability. Slight reduction of peak loads was sometimes detected after a large number of cycles but was judged to be of little consequence.

The load-deflection hysteresis curves, in general, resemble the well-known ones for the material itself.[2] It is noteworthy, however, that the hysteresis loops in Fig. 8 remained stable even after severe local buckling of the flanges had occurred. Such buckles were observed to appear and disappear cyclically, depending upon the sense of the applied load. Thus the beam and its connections were found to retain their load-carrying capacity even in the presence of pronounced buckling.

The hysteresis loops for bolted connections are unique. Slippage at the faying surfaces was responsible for the characteristic shape shown in Fig. 9. Three successive stages of structural action are discernible: static frictional resistance, active slip, and bearing on the bolts. The holes for specimens F3-C1 and F3-C5 were punched the customary $\frac{1}{16}$-in. oversize. Conversely, the holes for specimens F3A-C7 and F3B-C7, were drilled to a diameter of $\frac{41}{64}$-in., or $\frac{1}{64}$-in. over the nominal bolt size of $\frac{5}{8}$-in. As might be expected, the hysteresis loops for the latter two specimens exhibited a much smaller range of active slip, so that they approached the typical shape obtained for the other specimen types.

Figure 10 shows an example of hysteresis loops obtained for load versus the strain measured at a selected location. In the absence of buckling, these curves may be interpreted as moment-curvature relationships. It is then possible to compute the load-deflection hysteresis loops, using the area-moment method.[19] During the time of this investigation, unfortunately, facilities were not available for determining cyclic stress-strain relationships from coupon specimens.

General Behavior and Failure of Connections—It is well known that members and connections can be subjected to an extremely large number of load reversals without distress, provided that the elastic limit of the material is not exceeded. It appears that even if the elastic limit is exceeded slightly, the number of strain reversals before failure can still be very large. For example, specimen F1-C3 was subjected to 100 cycles with a tip-deflection of about 2.6 times its maximum elastic deflection. At the end of this sequence, no significant deterioration was noted, either in the hysteresis loops or visually in the specimen itself. An additional 20 cycles of much greater severity were required to fracture the specimen.

Unlike the experiment on specimen F1-C3, most of the tests were designed to produce failures with a smaller number of cycles. This was accomplished by increasing the cycling amplitude at predetermined increments in the number of cycles. With this in mind, several observations will now be made concerning the specimen failures.

A specimen was considered to have failed only when an increase in deflection was accompanied by a decrease in load, within the current cycling amplitude. There was some variation in the mode of failure, as can be seen in Figs. 11–14. Fracture was frequently in or near the welds, with several failures occurring in the groove welds of the flanges to the column face in the case of Type F1. Where there were welded connection plates, as in Types F2, W1 and W2, cracks usually initiated at the ends of the welds and propagated into the connecting plates. In severely strained connections, cracks would often be initiated at several locations and would then merge to precipitate complete fracture.

In some specimens, cracks were initiated or aggravated by the tack welds used to attach supplementary rotation instrumentation.[21] Sharp cornered web copes were a recurring source for initiation of web cracks. A few specimens failed due to complete fracture of a flange at a buckled cross section. In general, cracks propagated slowly as cycling progressed.

The behavior of the bolted connections was quite different from that of the welded ones. As noted previously, slippage between the plates and flanges was a characteristic phenomenon, and was often accompanied by loud bangs during testing. In connections with heavy connection plates, such as F3-C1 and F3-C5, failure occurred in the beam flanges at the bolt line farthest

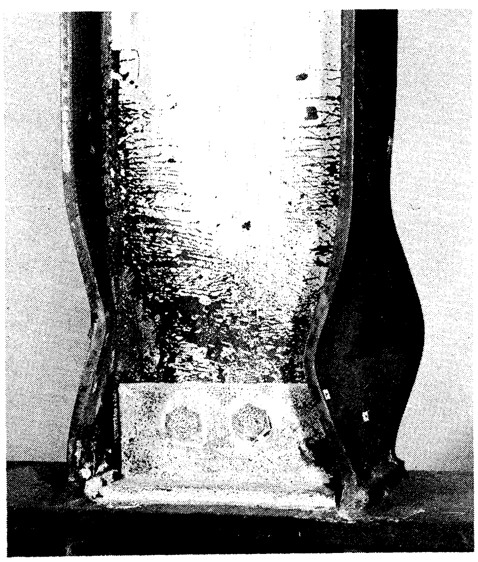

Fig. 11. Specimen F1HS-C11 at failure.

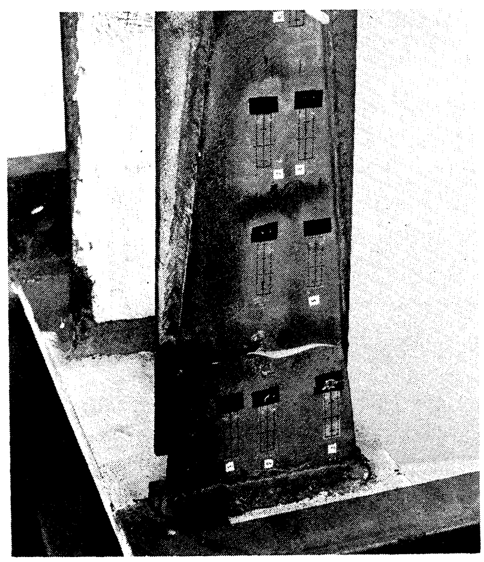

Fig. 12. Specimen F2-C1 at failure.

from the column. Thinner plates failed through the plates at the bolt line nearest the column.

Specimens W1-C1 and W1-C4 failed prematurely due to poor workmanship during fabrication. Contrary to design specifications, only about one-half of the flange thickness was beveled to receive the weld. Moreover, the beams were jammed tight against the connecting plates prior to welding, eliminating any root opening. The result was that the welds penetrated only one-half the flange thickness, rather than the entire thickness, as specified. In subsequent ultrasonic inspection, the indications produced by the unwelded contact surface were mistakenly interpreted as being due to the back-up bars.

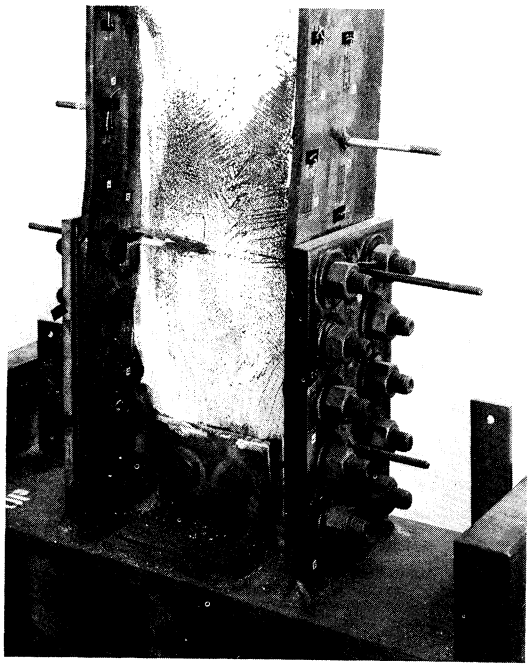

Fig. 13. Specimen F3-C1 at failure.

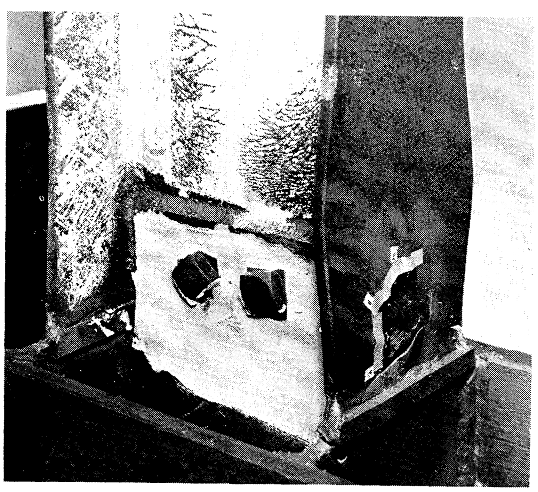

Fig. 14. Specimen W1-C9 at failure.

The possibility of such an inspection error appears less likely for thicker material. Nevertheless, shop inspection prior to welding, not performed for these two specimens, seems essential. The other web-connected specimens performed satisfactorily. The propensity for crack initiation in this type of connection appears, however, to be greater than in the flange-connected type.

Table 2 contains a brief description of each failure.

Table 2. Failure Descriptions

Specimen	Cycles to Failure	Description of Failure
F1-C1	28	Flange buckling; crack at buckle, bottom flange
F1-C2	22½	Flange buckling; crack near bottom flange weld
F1-C3	120	Flange buckling; crack at top flange weld
F1-C4	39½	Flange buckling; crack at stud at bottom flange buckle
F1-C6	32	Flange buckling; crack at top flange buckle
F2-C1	18	Crack in top plate at end of weld
F2-C4	44	Transverse crack in top plate at end of weld; longitudinal crack in top plate weld
F2A-C7	38½	Plates buckled near column; crack at bottom plate buckle
F2B-C8	32½	Bottom plate buckled near column; cracked at buckle and at weld
F3-C1	9½	Slight buckling of flanges; crack in top flange at outermost bolt line
F3-C5	30	Crack in top flange at outermost bolt line
F3A-C7	65½	First crack in bottom flange, outermost bolt line; second crack in top plate at innermost bolt line; actually simultaneous failure
F3B-C7	33½	Crack in bottom plate at innermost bolt line
W1-C1	5	Crack at top flange weld; defective welding
W1-C4	½	Crack at bottom flange weld; defective welding
W1-C7	37	Crack from end of top flange weld into plate
W1-C9	51½	Crack from end of bottom flange weld into plate
W2A-C7	46½	Buckling of bottom plate; crack initiated at cutting torch gouge in bottom plate
W2B-C10	30	Crack at weld in top plate
F1HS-C7	74	Flange buckling; crack at top flange weld
F1HS-C11	73	Flange buckling; crack near top flange weld
F2HS-C7	35½	Slight buckling of flanges; complete longitudinal crack of one top plate fillet weld
F2HS-C9	54½	Buckling of top flange and bottom plate; crack at bottom plate-to-column weld

DESCRIPTION OF RESULTS

The quantitative treatment of fatigue phenomena has traditionally been probabilistic in nature, due to the inherent impossibility of exactly reproducing material and geometric properties, and experimental technique, in two or more specimens. Such treatment requires, of course, a statistically valid number of experiments, with as nearly identical as possible input parameters. Thus, although the present problem can be characterized in part as one of low-cycle fatigue, the number and variety of specimens and the lack of uniformity of experiments preclude the use of a statistical approach. Fatigue theory, therefore, cannot be used, and rational analysis directed toward the prediction of such fatigue characteristics as expected life is not possible. The following analysis, then, will be largely qualitative, except insofar as actual experimental data are presented.

Design Parameters—Of primary concern to the designer are the strength and stiffness of a joint. Accordingly, the parameters which have been chosen to describe the design properties of a test specimen are the plastic load and the elastic stiffness, as computed from the actual geometry and material properties of the particular specimen, according to the specifications of the American Institute of Steel Construction. These parameters are represented schematically in Fig. 15. Figure 16 shows the parameters for all of the actual specimens, relative to the as-detailed properties of specimen type F1.

Nomenclature

- e Energy ratio for single excursion
- N Number of inelastic cycles to failure
- P Load
- P_p Plastic load
- r Ramberg-Osgood exponent
- W Energy dissipated during one excursion
- α Ramberg-Osgood parameter
- β Slope factor
- Δ Deflection
- Δ' Residual deflection
- Δ_p Elastic deflection corresponding to plastic load
- μ Ductility factor
- π_d Deflection plasticity ratio

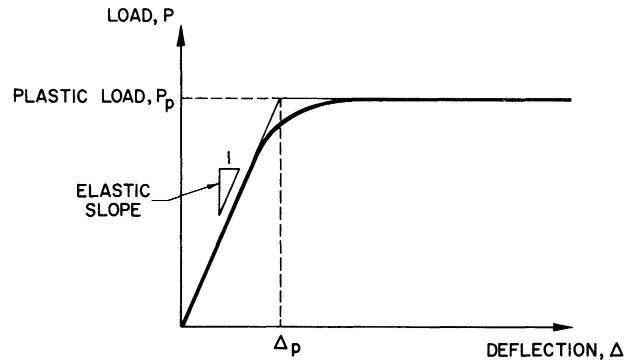

Fig. 15. Design parameters.

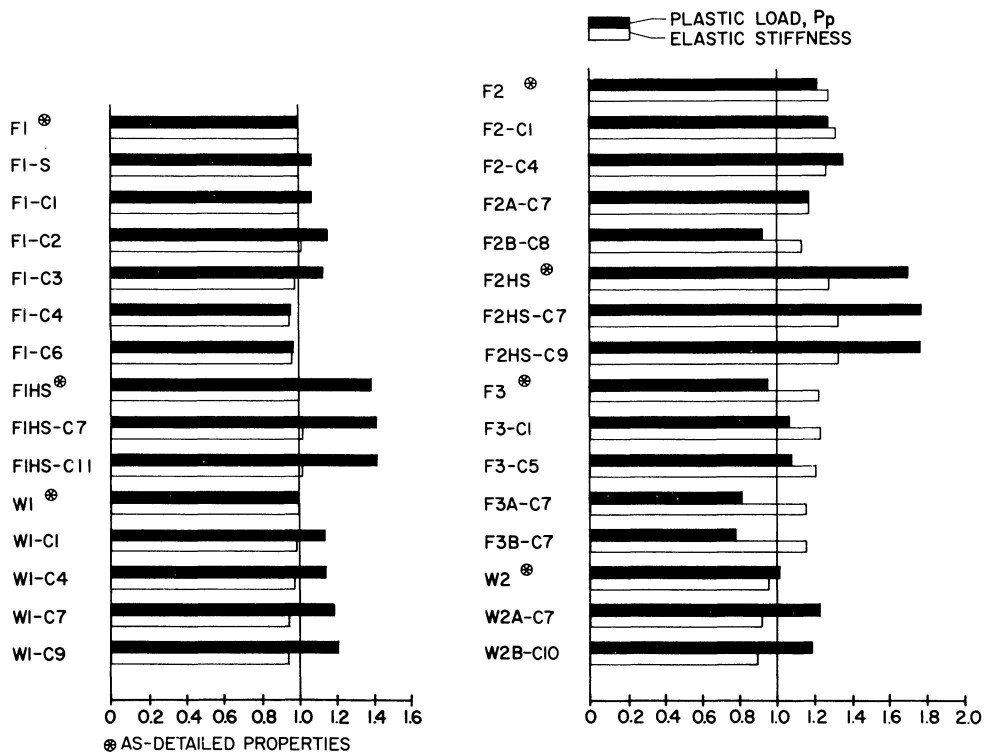

Fig. 16. Properties of specimens relative to Type F1.

Hysteresis Diagrams—The load-deflection hysteresis diagrams for a specimen contain considerable information about its performance. In addition to providing a continuous record of the relationship between load and deflection, the diagrams make it possible to determine the energy input to the specimen through integration of the work done by the external load.

Except for diagrams which display evidence of slippage, as do those for the Type F3 specimens, an analytical expression is available for the description of the typical nonlinear load-deflection relationship. Conceived by Ramberg and Osgood[22] for the description of nonlinear stress-strain curves, it has been adapted by Jennings[12], Kaldjian[14] and others to the present purpose and can be written

$$\frac{\Delta}{\Delta_p} = \frac{P}{P_p}\left[1 + \alpha\left|\frac{P}{P_p}\right|^{r-1}\right] \tag{1}$$

in which P and Δ = the load and deflection, respectively, while α and r are positive real numbers.

Equation 1 is the equation of the so-called "skeleton" or "back-bone" curve.[12,16] Iwan[11] has attributed to Massing (Masing[15]) the suggestion that the hysteresis curve is identical in shape to the skeleton curve, but enlarged by a factor of two. Following Masing's hypothesis, then, the related hysteresis curve can be generated by

$$\frac{\Delta - \Delta_i}{2\Delta_p} = \frac{P - P_i}{2P_p}\left[1 + \alpha\left|\frac{P - P_i}{2P_p}\right|^{r-1}\right] \tag{2}$$

The point (Δ_i, P_i) is chosen as the point of last load reversal. These relationships are shown[14] in Fig. 17. The geometrical implications of Eqs. 1 and 2 have been explored in detail elsewhere.[12,13]

Figure 18 shows a typical example of the close fit of the Ramberg-Osgood function to actual load-displacement relationships. Based on an analysis of many hysteresis diagrams, suggested values of the Ramberg-Osgood parameters are α = 0.5 and r = 8, for connections free of slip.

Ductility Factor—A widely used measure of the cyclic post-yield behavior of a structure is the so-called ductility factor, denoted by μ. Being the ratio of total deformation to elastic deformation at yield, it has been variously defined as that ratio for strains,[17] rotations,[11] and deflections.[5] The value of the ductility factor thus varies widely, depending upon the definition used. That for strain presumably depends almost exclusively on the material, while that for rotation adds the effects of the shape and size of cross section. When applied to deflections, the entire configuration of structure and loading is incorporated. Another source of confusion arises over whether the ductility factor is measured consistently from the initial configuration of the system, or from the immediately preceding no-load configuration. Thus, in any analysis of the ductility factor, it is important to bear in mind the definition used. Moreover, it becomes difficult to generalize on the adequacy, or lack thereof, of the ductility so measured.

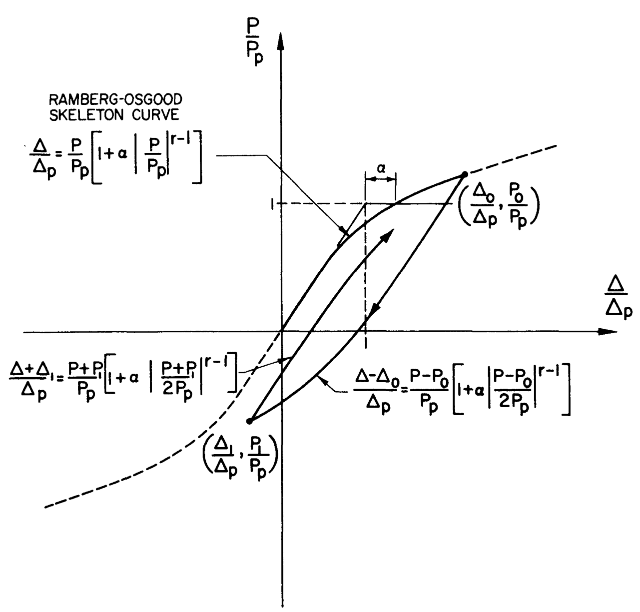

Fig. 17. Masing's hypothesis applied to Ramberg-Osgood function.

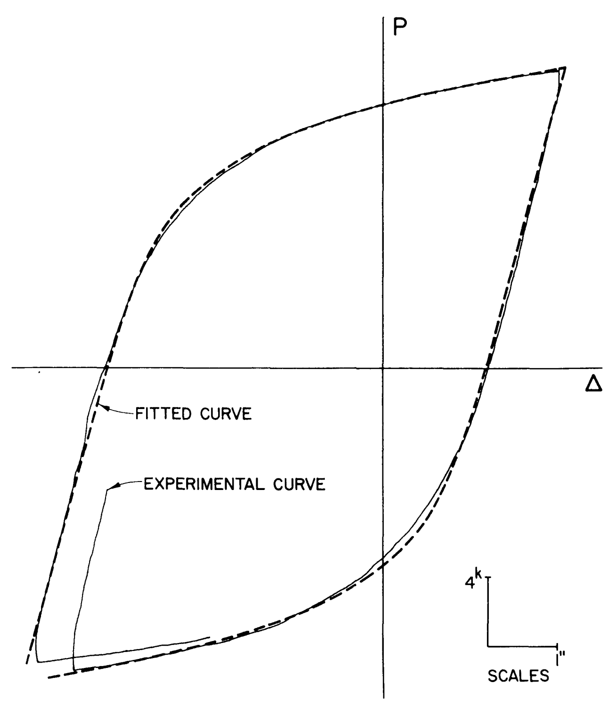

Fig. 18. Example of least-squares fit—specimen F1-C2.

Plasticity Ratio—The previous definition of the ductility factor is perhaps unfortunate; it includes the recoverable deformation as well as the permanent, or plastic, deformation. It is thus awkward to use as a cumulative damage indicator. Furthermore, it is best suited to steady-state response, as it is otherwise inconvenient to keep track of the residual displacement at no load. A more logical measure would seem to be the ratio of residual plastic deformation to elastic deformation at yield. This ratio will be defined herein for deflections and will be referred to as the "deflection plasticity ratio," or simply the "plasticity ratio," denoted by π_d. By restricting the definition in this way, the ambiguities associated with the ductility factor, as outlined previously, can be completely avoided. Fig. 19 defines the ductility factor μ and plasticity ratio π_d as used herein.

The magnitude of the plasticity ratio or ductility factor which could be achieved was found to be simply a matter of how much deflection was applied to the beam. The maximum values applied to the specimen are given in Table 3. It is emphasized that these are maximum values applied. In no case should it be construed that an entire test was conducted with the tabulated value; nor should it be construed that larger values could not be attained for any specimen.

Cyclic Energy Dissipation—The dynamic response of a structure is markedly influenced by the amount of energy absorbed and dissipated during motion. Since response is usually described in terms of displacement, it is of interest to know how the cyclic energy dissipation is

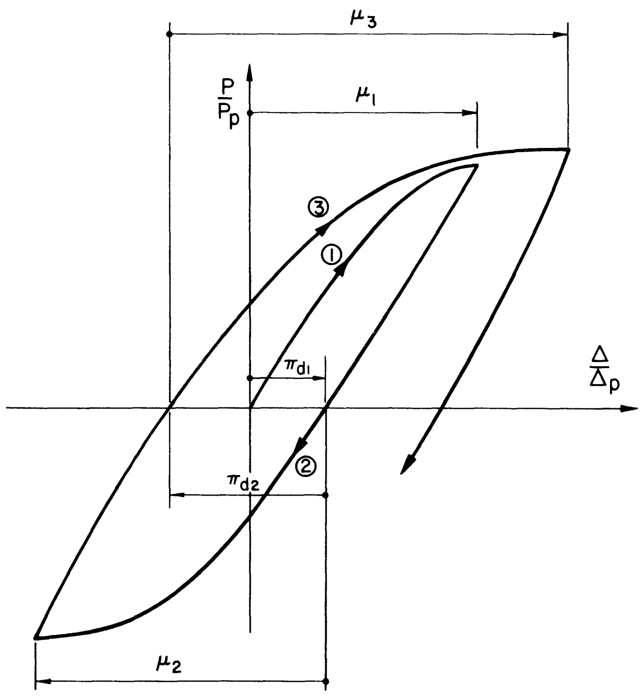

Fig. 19. Definition of ductility factor μ and plasticity ratio π_d.

Table 3. Maximum Applied Ductility Factors and Plasticity Ratios

Specimen	$(\pi_d)_{max}$	μ_{max}	Specimen	$(\pi_d)_{max}$	μ_{max}
F1-C1	12.2	13.9	F3A-C7	12.7	14.8
F1-C2	12.3	13.8	F3B-C7	8.3	9.8
F1-C3	8.3	9.7	W1-C1	2.2	3.5
F1-C4	9.5	11.2	W1-C7	3.4	5.0
F1-C6	14.5	16.1	W1-C9	4.8	6.2
F2-C1	9.8	11.3	W2A-C7	4.6	5.8
F2-C4	5.7	7.2	W2B-C10	3.6	4.8
F2A-C7	5.0	6.3	F1HS-C7	5.8	7.4
F2B-C8	7.3	8.5	F1HS-C11	6.0	7.2
F3-C1	13.3	15.0	F2HS-C7	3.0	4.2
F3-C5	11.8	13.4	F2HS-C9	4.8	6.2

related to displacement. Jennings[13] has shown this relationship in terms of total displacement for steady-state response, and based on the Ramberg-Osgood hysteresis shape. Once again, however, the random nature of earthquake response makes it inconvenient to employ the total displacement in this manner. Therefore, the permanent deformation, as incorporated into the previously defined deflection plasticity ratio π_d, will be used.

It is convenient to define a dimensionless energy ratio $e = W/[(\frac{1}{2})P_p\Delta_p]$ based on the energy dissipated during a single excursion. Figure 20 shows the relationship be-

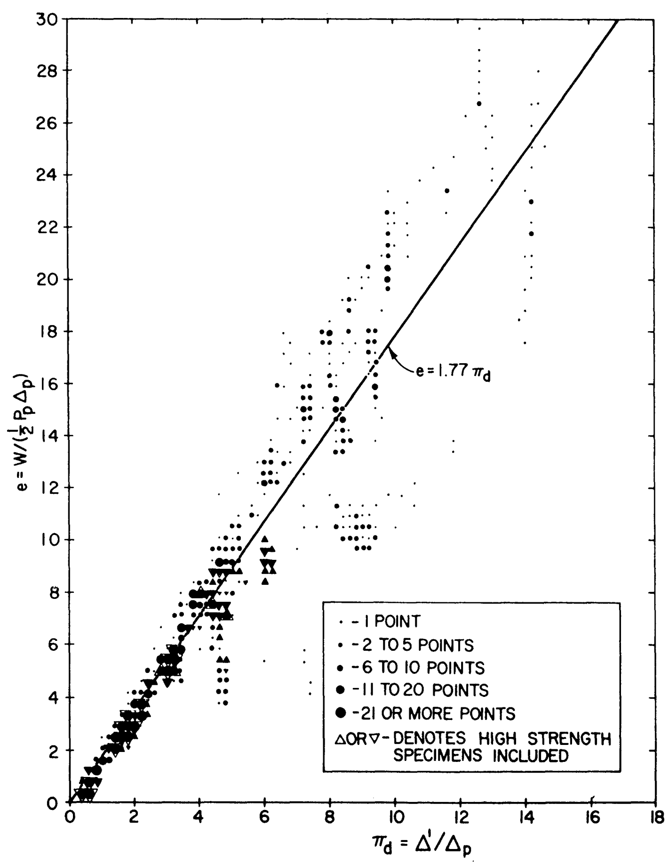

Fig. 20. Energy ratio vs. plasticity ratio.

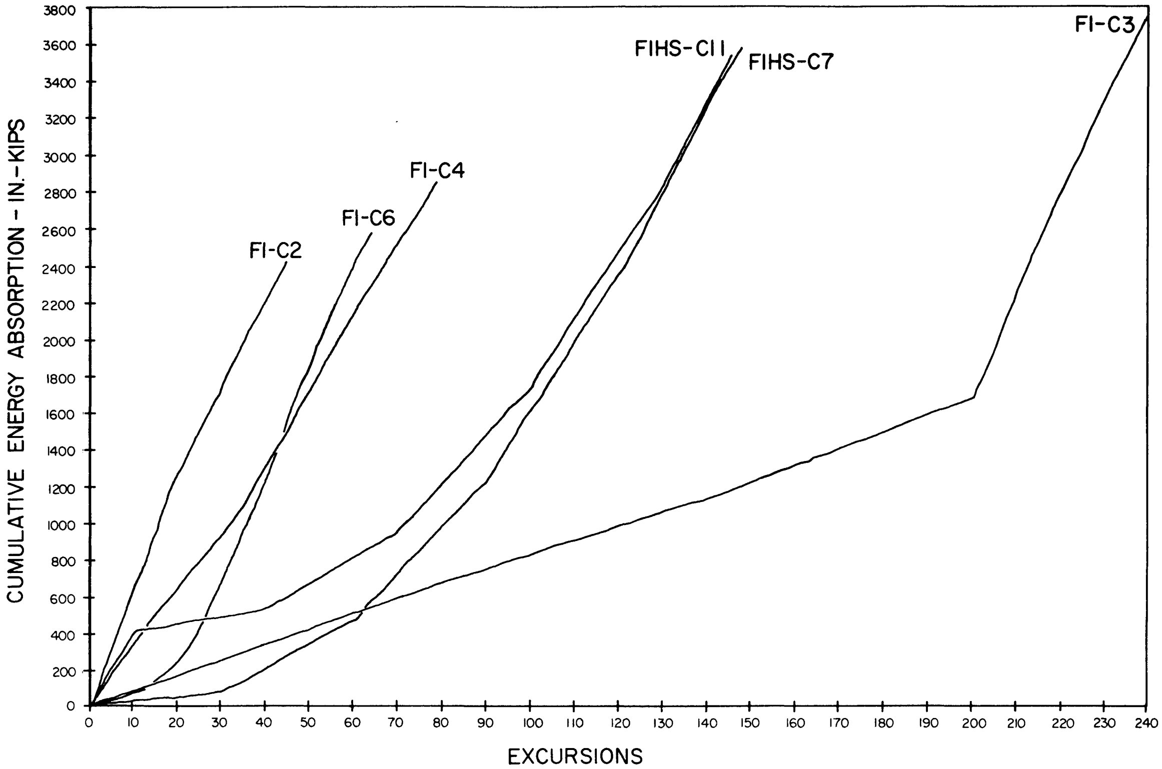

Fig. 21. Cumulative energy absorption.

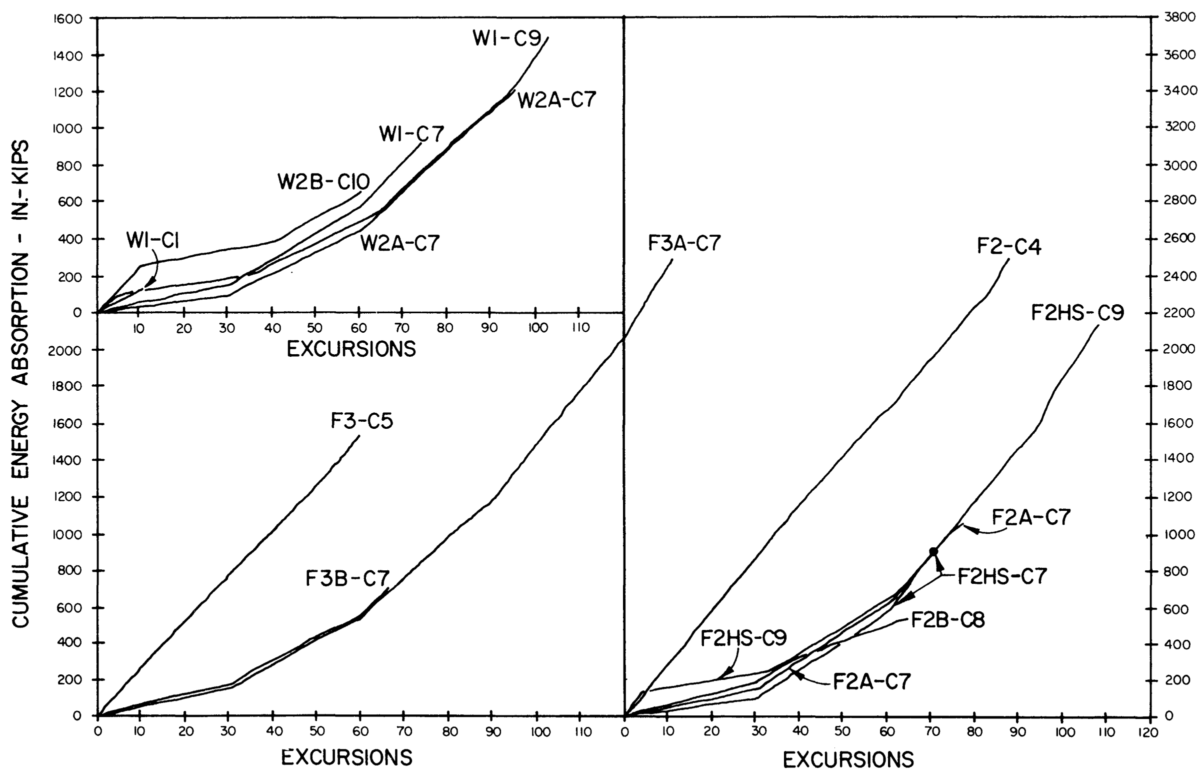

Fig. 22. Cumulative energy absorption.

tween e and π_d for each excursion for every specimen, including those of Type F3, for which energy data were available. A total of 1,730 points have been plotted; points enclosed by triangles include data for the A441 specimens.

It may be noted that for low values of π_d, the points are well clustered near the least-squares fitted line. It has been suggested elsewhere[8] that a ductility factor of the order of 4, corresponding to a plasticity ratio of about 3, might be experienced in a structure. If so, then the lowermost portion of the diagram of Fig. 20 would be by far the most significant. Thus the line shown is proposed as a reasonable estimate for relating the energy absorption to the plastic displacement for at least the two types of steel tested.

Cumulative Energy Dissipation—Energy dissipation has been suggested as a criterion of cumulative damage.[17] One way to describe the history of a specimen, then, is to plot the cumulative energy absorption throughout that history. Figures 21 and 22 show these data for all specimens. The slope of each curve indicates the rate of energy absorption, while its terminus indicates the point at which failure occurred. Both the total energy and the number of excursions to failure can be read from this point.

It will be noticed that the Type F1 specimens show consistently high energy absorbing capabilities, even at high rates of absorption. Furthermore, the specimens of both types of steel performed well. Conversely, a higher rate of absorption generally led to a shorter life.

On the whole, none of the other specimen types performed as well as F1, in terms of actual energy absorption capability. Again, however, in the case of Type F2, no superiority of one steel over the other could be discerned. A particularly interesting aspect of the general performance is illuminated by a consideration of the Type F3 specimens. The plates of specimen F3-C5 developed the strength of the gross section of the beam, while those of specimen F3B-C7 developed only the strength of the net section (refer to Table 1). As might be expected, failure (i.e., opening of a crack) occurred in F3-C5 at the net section of the beam, and in F3B-C7, at the net section of the plates. Conversely, the plates of specimen F3A-C7 developed a strength intermediate between those of the gross and net sections of the beam. Here, failure occurred simultaneously at the net section of both beam and plates. This specimen was able to sustain a considerably larger energy input than either of the other two, leading to the conclusion that the greater the volume of material over which the damage can be spread, the longer the life of the specimen. The better performance of the Type F1 specimens can therefore presumably be attributed to the severe flange buckling, while damage was necessarily more localized in the plated connections. This would also account, at least in part, for the somewhat less satisfactory performance of the W-type connections, in that the stress concentrations resulting from their configurations once again localized the damage. It is concluded that, in general, a relatively stiffer connection will suffer in comparison with another more flexible one of the same strength.

Total Energy Dissipation—The total energy dissipated by each specimen can be read from Figs. 21 and 22, as previously explained. It is possible, however, to present the failure points in terms of the accumulated energy ratio Σe and the accumulated plasticity ratio $\Sigma\pi_d$, where each summation is carried out over the total number of excursions for each test. These data are shown in Fig. 23.

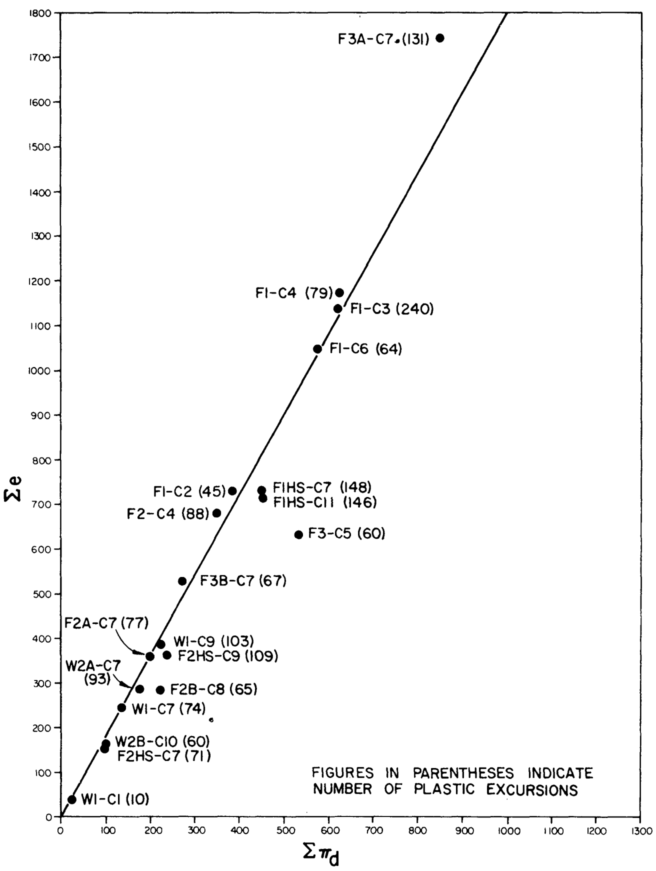

Fig. 23. Accumulated energy ratio vs. accumulated plasticity.

Figure 23 suggests that the total energy ratio at any time in the history of a specimen is simply related to the total plasticity ratio as accumulated to that time. Thus, if the history of plastic deformation of a connection is known, it is possible to obtain some idea of its expected life, if it is at all similar to any of the specimen configurations tested. Obviously, this procedure is extremely subject to the interpretation of the designer or analyst and is qualitative only.

CONCLUSIONS

Based on the results of this investigation, a number of conclusions can be reached. Some of these are of immediate significance to the designer; others may be of importance for future research.

1. The load-deflection hysteresis loops for a steel cantilever beam and connection are highly reproducible during repetitive load application. This implies that such an assemblage is very reliable, and can be counted upon to absorb a definite amount of energy in each cycle for a prescribed displacement.

2. Using total energy absorption as the sole criterion, the performance of specimen type F1 in general excelled that of any other type. No clear superiority was apparent among the other types of connection. All sustained loads in excess of their design limit loads until the onset of cracking.

3. The ability to withstand severe repeated and reversed loading seems to be assured for properly designed and fabricated steel connections; their intrinsic energy absorption capacity is large. Moreover, the number of repeated and reversed loadings which can be safely sustained appears to be in excess of that which may be anticipated in actual service, although this requires justification by means of a dynamic analysis of buildings subjected to seismic action.

4. The performance of specimens of A441 steel was comparable to that of specimens of A36 steel. In the specimens tested, higher loads were developed because of geometric similarity. Energy absorption capability was as good as or better than that for A36 steel. The choice of steel depends upon the particular application.

5. The importance of careful inspection during fabrication was brought out by the premature failure of two improperly welded connections.

6. It has been demonstrated that flange local buckling did not precipitate an immediate loss of load-carrying capacity. Indeed, the ability to buckle and thus distribute damage may be of significance in prolonging the life of a member. Such distribution of damage, or lack thereof, has been related qualitatively to the respective longevities of the specimens tested.

7. The energy absorption capacity, as measured by the size of the hysteresis loops, increases with increasing tip deflection. A simple linear dependence of the dissipated energy per cycle upon the residual deflection has been suggested.

8. The plasticity ratio has been defined and proposed as a more useful measure of post-yield performance than the ductility factor.

9. The mathematical representation of a hysteresis curve using the Ramberg-Osgood relationship has been found to be highly satisfactory, in the absence of slip, justifying its use in analysis of structures subjected to inelastic load reversal.

10. It does not appear possible on the basis of these tests to formulate a rational approach to the prediction of total energy absorption capacity. Only a qualitative assessment may be made by means of direct comparison with actual test results.

Finally, it must be emphasized that this paper is based entirely on a single beam size, 8W20. Extrapolation to members with other cross sections must be done with caution.

ACKNOWLEDGMENTS

The writers wish to acknowledge with gratitude, the financial support of the American Iron and Steel Institute, and the technical advice of the AISI Advisory Committee and the Committee on Seismology of the Structural Engineers Association of California under the chairmanship of C. A. Zwissler. During the course of the investigation, carried out at the University of California, Berkeley, graduate students H. A. Franklin, D. W. Murray, and M. C. Chen, and undergraduate student J. V. Meyer provided valuable assistance. The continued interest and encouragement of I. M. Viest, member of the AISI Engineering Subcommittee on Earthquake Research, was much appreciated.

REFERENCES

1. *Beedle, L. S., et al.* Structural Steel Design (*L. Tall, ed.*), *The Ronald Press Co., New York, 1964.*
2. *Benham, P. P., and Ford, H.* Low Endurance Fatigue of a Mild Steel and an Aluminum Alloy, *Journal of Mech. Eng. Science, Vol. 3, No. 2, June, 1961, pp. 119–132.*
3. *Bertero, V. V., and Popov, E. P.* Effect of Large Alternating Strains on Steel Beams, *Journal of the Structural Division, ASCE, Vol. 91, No. ST1, February, 1965, pp. 1–12.*
4. *Blume, J. A., Newmark, N. M., and Corning, L. H.* Design of Multi-Story Reinforced Concrete Buildings for Earthquake Motions, *Portland Cement Association, Skokie, Ill., 1961.*
5. Commentary on Plastic Design in Steel, Manual of Engineering Practice No. 41, *New York, 1961.*
6. *Douty, R. T., and McGuire, W.* High Strength Bolted Moment Connections, *Journal of the Structural Division, ASCE, Vol. 91, No. ST2, Proc. Paper 4298, April, 1965, pp. 101–128.*
7. *Hodge, P. G., Jr.* Plastic Analysis of Structures, *McGraw-Hill Book Co., New York, 1959.*
8. *Hanson, N. W., and Conner, H. W.* Seismic Resistance of Reinforced Concrete Beam-Column Joints, *Journal of the Structural Division, ASCE, Vol. 93, No. ST5, Proc. Paper 5537, October, 1967, pp. 533–560.*
9. *Hanson, R. D.* Comparison of Static and Dynamic Hysteresis Curves, *Journal of the Engineering Mechanics Division, ASCE, Vol. 92, No. EM5, Proc. Paper 4949, October, 1966, pp. 87–113.*
10. *Igarashi, S., Sumida, J., and Sakamoto, J.* Experimental Study on the Hysteresis Characteristics of Steel Connections with Relation to the Damping Properties of a Structure, *Transactions, Architectural Institute of Japan, Vol. 75, August, 1962.*

11. *Iwan, W. D.* On a Class of Models for the Yielding Behavior of Continuous and Composite Systems, *Journal of Applied Mechanics, ASME, Vol. 34, No. 3, September, 1967, pp. 612–617.*
12. *Jennings, Paul C.* Periodic Response of a General Yielding Structure, *Journal of the Engineering Mechanics Division, ASCE, Vol. 90, No. EM2, Proc. Paper 3871, April, 1964, pp. 131–166.*
13. *Jennings, Paul C.* Earthquake Response of a Yielding Structure, *Journal of the Engineering Mechanics Division, ASCE, Vol. 91, No. EM4, Proc. Paper 4435, August, 1965, pp. 41–68.*
14. *Kaldjian, M. J.* Moment-Curvature of Beams as Ramberg-Osgood Functions, *Journal of the Structural Division, ASCE, Vol. 93, No. ST5, Proc. Paper 5488, October, 1967, pp. 53–65.*
15. *Masing, G.* Eigenspannungen und Verfestigung beim Messing, *Proceedings of the Second International Congress for Applied Mechanics, Zurich, September, 1926.*
16. *Medearis, K., and Young, D. H.* Energy Absorption of Structures Under Cyclic Loading, *Journal of the Structural Division, ASCE, Vol. 90, No. ST1, Proc. Paper 3791, February, 1964, pp. 61–91.*
17. *Morrow, Jo Dean* Cyclic Plastic Strain Energy and Fatigue of Metals, *Internal Friction Damping and Cyclic Plasticity, ASTM, STP-378, 1965, p. 77.*
18. *Naka, T., Kato, B., Watabe, M., Tanaka, A., and Sasaki, T.* Research on the Behavior of Steel Beam-to-Column Connections Subjected to Lateral Force—Report No. 3, *Transactions of the Architectural Inst. of Japan, Vol. 103, October, 1964.*
19. *Popov, E. P.* Low-Cycle Fatigue of Steel Beam-to-Column Connections, *International Symposium on the Effect of Repeated Loading on Materials and Structures, RILEM-Instituto de Ingeneria, Vol. VI, Mexico City, September, 1966.*
20. *Popov, E. P., and Pinkney, R. B.* Behavior of Steel Building Connections Subjected to Repeated Inelastic Strain Reversal, *Report No. SESM 67-30, Structural Engineering Laboratory, University of California, Berkeley, December, 1967.*
21. *Popov, E. P., and Pinkney, R. B.* Behavior of Steel Building Connections Subjected to Repeated Inelastic Strain Reversal—Experimental Data, *Report No. SESM 67-31, Structural Engineering Laboratory, University of California, Berkeley, December, 1967.*
22. *Ramberg, W., and Osgood, W. R.* Description of Stress-Strain Curves by Three Parameters, *Technical Note 902, NACA, July, 1943.*
23. *Symonds, P. S., and Neal, B. G.* Recent Progress in the Plastic Methods of Structural Analysis, *Journal of the Franklin Institute, Vol. 252, 1951, pp. 383–407 and 469–492.*